International Journal of Engineering Research & Technology (IJERT)
ISSN: 2278-0181
Vol. 3 Issue 8, August - 2014

Numerical Study of Flow and Heat Transfer in Circular Tube With Almond Shape Dimple

Pooja Patil[1], Prof. Padmakar Deshmukh[2]
Mechanical Engg. Department, University of Pune
Rajarshi Shahu College of Engg. Pune, India.

Abstract:- This paper presents Computational investigation of convective heat transfer in turbulent flow past an almond shape dimpled surface. A parametric study is performed with k-ε turbulence model to determine the effects of Reynolds number of range 25000 to 95000 on heat transfer enhancement. In this paper we have computed heat transfer characteristics in a circular tube as a function of the Reynolds number. The mass flow rate of air varied for getting turbulent flow Reynolds numbers. The almond shape dimple geometry was considered with diameter 10 mm and required elongated length 22.5mm. The tube diameter 19mm and dimple depth 3mm with ratio L/D =4.3 was kept constant. . The results showed that more heat transfer was occurred downstream of the dimples due to flow reattachment. As the Reynolds number increased, the overall heat transfer coefficient was also increased as compared with base line plain tube with minimum pressure drop penalty.

Keywords: Almond shape dimples, Turbulent Flow, Reynolds number, Circular tube, Heat transfer coefficient

1. INTRODUCTION

A great deal of research effort has been devoted to developing apparatus and performing experiments to define the conditions under which an enhancement technique will improve heat transfer. Heat transfer enhancement technology has been widely applied to heat exchanger applications in refrigeration, automobile, process industries etc. The goal of enhanced heat transfer is to encourage or accommodate high heat fluxes. The need to increase the thermal performance of heat exchangers, thereby effecting energy, material and cost savings have led to development and use of many techniques termed as heat transfer augmentation. These techniques are also referred as Heat Transfer Enhancement or Intensification. Augmentation techniques increase convective heat transfer by reducing the thermal resistance in a heat exchanger.

In order to improve the heat transfer efficiency and operation safety of heat transfer equipments, many techniques have been proposed , such as treated surfaces, rough surfaces, extended surfaces, swirl flow devices, shaped pipes, surface tension devices, technical aids, electrostatic fields, suction or injection. However, all of the above techniques will inevitably bring too much flow resistance, resulting in unnecessary power consumption. An effective method of heat transfer enhancement is required to not only improve the heat transfer greatly, but also minimize the flow resistance as much as possible. In recent years, the concept of using an indented (dimpled) surface instead of protruding devices has gained attention because of the combination of high heat transfer enhancement and a lower pressure loss penalty.

Johann Turnow *et al.* Studied Vortex structures and heat transfer enhancement mechanism of turbulent flow over a staggered array of dimples in a narrow channel. It was found that the dimple package with a depth h to diameter D ratio of h/D = 0.26 provides the maximum thermo-hydraulic performance. The heat transfer rate could be enhanced up to 201% compared to a smooth channel [1]. Yu Rao *et al*. investigate the effects of dimple depth on the pressure loss and heat transfer characteristics in a pin fin-dimple channel, where dimples are located on the end wall transversely between the pin fins. The study showed that, compared to the baseline pin fin channel, the pin fin-dimple channels have further improved convective heat transfer performance by up to 19.0%, and the pin fin-dimple channel with shallower dimples shows relatively lower friction factors by up to 17.6% over the Reynolds number range 8200 to 50,500[2]. C. Bi *et al*. studied convective cooling heat transfer in mini-channels with dimples, cylindrical grooves and low fins. The results show that the dimple surface presents the highest performance of heat transfer enhancement [3]. Chyu *et al*. studied the enhancement of surface heat transfer in a channel using two different concavities- hemispheric and tear drop. Concavities serve as vortex generators to promote turbulent mixing in the bulk flow to enhance the heat transfer at Re no.= 10,000 to 50,000, H/d of 0.5, 1.5, 3.0 and δ /d =0.575. Heat transfer enhancement was 2.5 times higher than smooth channel values and with very low pressure losses that were almost half that caused by conventional ribs turbulators [13].S.A. Isaev studied Influence of the Reynolds number and the spherical dimple depth on turbulent heat transfer and hydraulic loss in a narrow channel. Detailed information gained from the presented computations can be used to get a deep insight into flow physics over dimpled surfaces and as a benchmark for validation of numerical and experimental methods [4].

IJERT

(This work is licensed under a Creative Commons Attribution 4.0 International License.)

Jonghyeok Lee wt *et al*. developed Correlations and shape optimization in a channel with aligned dimples and protrusions. The friction factor and Nusselt number in a plate heat exchanger with dimples and protrusions were investigated according to geometric and operating conditions[5].Somin Shin *et al*. were measured Heat transfer coefficients in a channel with one side dimpled surface.The sphere type dimples were fabricated for the different diameter channel heights. The Reynolds number based on the channel hydraulic diameter was varied from 30000 to 50000. Heat transfer measurement results showed that high heat transfer was induced downstream of the dimples due to flow reattachment. Due to the flow recirculation on the upstream side in the dimple, the heat transfer coefficient was very low. As the Reynolds increased, the overall heat transfer coefficients also increased. With the same dimple arrangement, the heat transfer coefficients and the thermal performance factors were higher for the lower channel height. As the distance between the dimples became smaller, the overall heat transfer coefficient and the thermal performance factors increased [6]. Yu Rao *et al.* An experimental and numerical study was conducted to investigate the flow friction and heat transfer performance in rectangular channels with staggered arrays of pin fin-dimple hybrid structures and pin fins in the Reynolds number range of 8200–54,000.Experimenta and numerical compared data showed that, compared with the pin fin channel, the pin fin-dimple channel has further improved convective heat transfer performance by about 8.0% and whereas lowered flow friction by more than 18.0%.The computations showed that the dimples increase the near-wall turbulent mixing level by producing strong vortex flows, and therefore enhance the convective heat transfer in the channel. On the other hand, the dimples enlarge the minimum cross section area transversely between the pin fins, and therefore the pressure loss in the flow can be reduced in the pin fin-dimple channels.[7] Yu Chen studied a systematic numerical investigation of heat transfer in turbulent channel flow over dimpled surface .The tow dimple configurations were studied that is symmetric and asymmetric, for h/d. It was found that the heat transfer enhancement would be 15% for asymmetric h/d with minimum loss of pressure as compare to symmetric dimples [8]. Nopparat Katkhaw *et al*. studied the Heat transfer behavior of flat plate having45^0 ellipsoidal dimpled surfaces. 10 types of dimple arrangements and dimple intervals are studied. For the staggered arrangement of dimple it was found that 15.8% heat transfer was improved as compare to smooth channel [9]. M. Siddique *et al.* made a review article for the recent advances in heat transfer enhancement [10].

From the published literature, it can be seen that there is a lot of experimental and numerical data available on the use of dimpled surfaces. However, there is a scarcity of literature available for computational work in the Turbulent flow regime inside circular tube. There is a need to gain a better insight in to the nature of Turbulent flows over dimpled surface. An investigation to see the effects of different array geometries is also needed. This study is carried out to see whether almond shape dimples can enhance heat transfer and thermal performance for turbulent airflows in a circular channel for two different array geometries using Computational fluid dynamics.

2. DATA REDUCTION

The area averaged convective heat transfer coefficient of the test channel is defined by:

$$h = \frac{Q_{net}}{A_s \Delta T_{lm}} = \frac{m C_p (T_o - T_i)}{A_s (\Delta T_{lm})} \quad (1)$$

Here Q_{net} is the enthalpy change of an air and A_s is the wall surface area of the test tube and ΔT_{lm} the log mean temperature difference between the heating wall and the cooling flow.

The log mean temperature difference between the heating wall and the cooling flow, DTlm, is calculated based on the equation below:

$$T_{lm} = \frac{(T_w - T_{in}) - (T_w - T_o)}{ln \frac{(T_w - T_{in})}{(T_w - T_o)}} \quad (2)$$

The area averaged Nusselt number is based on the hydraulic diameter, and it is defined by:

$$Nu = \frac{hD_i}{k} \quad (3)$$

The Nusselt number by Dittus Boelter equation:

$$Nu = 0.023 Re^{0.8} Pr^{0.4} \quad (4)$$

The pressure drop of the airflow across the test channel, L is the length of the test channel

$$Pressure\ Drop = \frac{4 f l \rho v^2}{2D} \quad (5)$$

$$Enhancement\ Factor = \frac{Enthalpy\ change\ of\ dimple\ tube}{Enthalpy\ change\ of\ plain\ tube} \quad (6)$$

Enhancement efficiency can be defined as the ratio of heat transfer coefficient of dimple tube to the heat transfer coefficient of tube without dimple

$$Enhancement\ Efficiency: \eta = \frac{h}{h_0} \quad (7)$$

The thermal performance factor is calculated using the following equation. This factor gives the thermal performance per unit pumping power by the dimpled

IJERT

(This work is licensed under a Creative Commons Attribution 4.0 International License.)

surface in comparison to the thermal performance per unit pumping power in case of the plain tube.

$$Thermal\ performance\ factor\ T_{pf} = \frac{\frac{Nu}{Nu_0}}{(\frac{f}{f_0})^{1/3}} \quad (8)$$

Reynolds number:

$$Re\,no. = \frac{\rho v D}{\mu} \quad (9)$$

[14]

3. COMPUTATIONAL SET UP

For problems associated with Fluid Mechanics and Heat Transfer, CFD can be used to solve the Navier-Stokes equations which are a coupled set of partial differential equations for which no closed form analytical solution has been found till date. The solution of Navier-Stokes equations for different fluid and thermal systems depends on the numerical application of boundary conditions for that particular system. With the advancement of computer resources and continuous research on development of efficient solution methods, many problems which were considered complex can be easily solved with the use of CFD. In spite of all these advantages of CFD, it should be remembered that CFD cannot replace pure theory and pure experiment and that it can be only used to validate analytical and experimental results. This is because of the fact that many problems cannot be realistically modeled using CFD even today and that realistic solutions can only be found by theory or experiment. The process of solving a problem using CFD consists of the following steps in general.

3.1CFD Analysis

Problem Definition:

In this work, a numerical investigation was carried out to see the effects of almond shape dimple arrays on heat transfer characteristics in a tube. These effects were observed for dimples on the wall of the tube for turbulent airflows. The effects of a staggered array and a inline array on the wall were investigated using a 3D steady viscous computational fluid dynamics package with an unstructured grid. The heat transfer characteristics were studied as a function of the Reynolds number based on the hydraulic diameter of the tube. The tube diameter and dimple depth ratio was kept constant, while holding diameter 0.005m of dimple is required length 0.0215 m because of the elongated shape. The heat transfer was quantified by computing the average heat transfer coefficient and Nusselt number. The pressure drop and flow characteristics were also calculated. The Nusselt number was compared with that of a plane tube without dimples to assess the level of heat transfer enhancement provided by the dimple. This investigation was carried out to observe if the use of dimples in a tube can enhance heat transfer characteristics without severe penalties associated with pressure drops for turbulent airflows. When compared with a plane tube, the use of dimples enhanced heat transfer. It was also observed that the staggered array facilitates higher heat transfer augmentation when compared to the inline array.

3.2 Computational Procedure:

The computation is performed with FLUENT Version14.5 The tube and almond shape dimple geometries employed in the computation are exactly the same as those used in the experiments. The meshing is done using GAMBIT. The numbers of the grid nodes range from about 0.5 to1.35×10^3, depending on the dimple geometry and grid independence studies. Fine meshes are generated inside the dimples and around the edges of dimples to resolve key features in the vicinity of the dimple. The problem is modeled as a steady, 3-dimensional heat transfer problem with a uniform wall temperature. The k-ε model is employed for the calculations. This turbulence model represents the most sophisticated model available for turbulent flow calculations in FLUENT. During the computation, the tube wall is set to the constant wall temperature The uniform inlet velocity is determined by selecting the inlet Reynolds number Re15,000.The temperature of the main flow is set to be 303 K, and the wall temperature is set to be 353 K. Because the temperature difference is only 323 K, and the main stream velocity is low (less than 10 m/s), the velocity field is assumed to be independent of temperature.

3.3 Model Geometry:

The fluid flow area inside the tube was modeled using the commercial CAD software CATIA. To model dimples inside the tubes, shapes were created on the surface of tube with two different array geometries. An inlet section with length same as the heated tube was created to ensure fully developed flow conditions while an outlet section also with the same length of the heated section. The heated part has of the alternating 2 rows; while the inline array had 9 dimples in each row. The dimple depth is 3mm,with diameter 10 mm and length is 22.5mm.Length to diameter ratio is kept constant in each array L/D=4.3,Where tube is 19mm diameter and 1000 mm length dimensions. The staggered array had 9 and 8 dimples in pitch is 100mm.

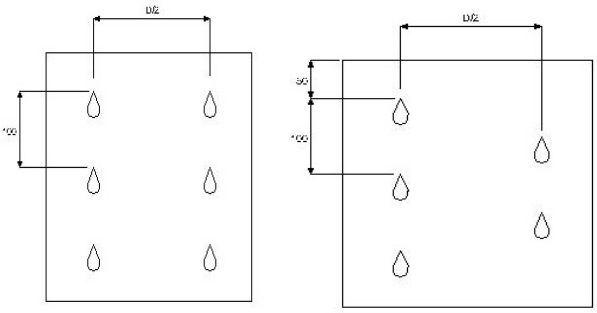

Fig.1: Geometrical configuration of aligns and staggered dimple

IJERT

(This work is licensed under a Creative Commons Attribution 4.0 International License.)

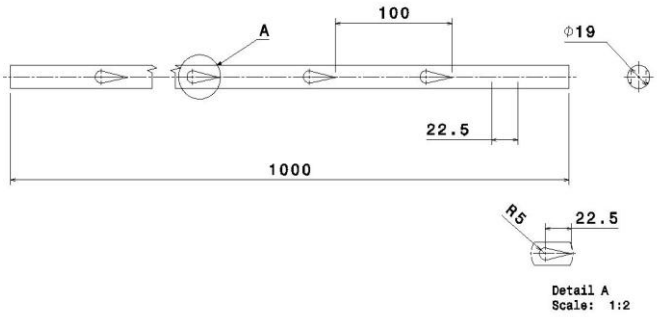

Fig.2: Geometrical Configuration of Test tube

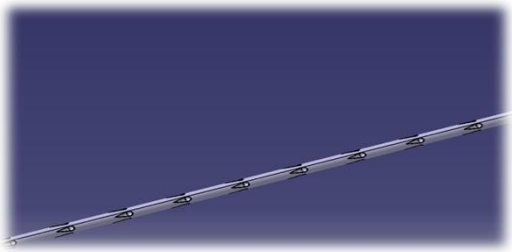

Fig.3:Tube with Almond shape dimples

3.4 Grid generation:

Gambit was used for meshing the computational domain. A mixed tetrahedral prism mesh was generated. The grids selected for the geometries are given in Table. The given geometry is approximately the same as per studied computation.

Table 1: Grids selected for various geometries

Geometry	***Number of elements***
Plain tube	1,20,000
Staggered array	1,35,000
Inline array	1,35,000

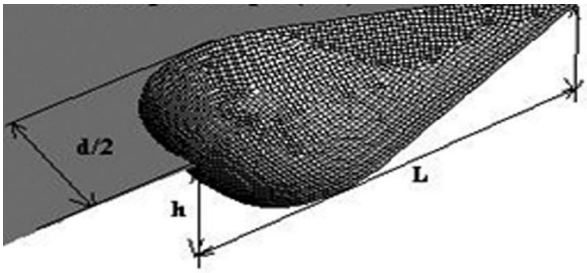

Fig.4: Geometry of the dimple [12]

3.5 Solution Setup:

The commercial CFD software Fluent 14.5 was used for the computational solution. The mesh was read in to Fluent and setup for solution.

• **Solver**:

The pressure based segregated implicit solver was selected for the solution. The pressure based solver is typically used for low speed incompressible flows and hence was selected for the present study

• **Material properties and flow conditions**:

Air was the fluid material selected for flow inside the channel. The turbulent viscous k-ε reliable model was used to Material Properties model the flow conditions. The material properties of air are given in the table.

Table 2: Material properties of air

Property	***Value***
Density of air	1.225 kg/m^3
Specific heat	1006.43 J/kgK
Thermal Conductivity	0.242 W/mK
viscosity	1.789×10^{-5} Pa

Table 3: Material properties of aluminum

Property	***Value***
Density	2719 kg/m^3
Specific heat	871 J/kgK
Thermal conductivity	202.4 W/mK

3.6 Boundary Conditions:

Correct numerical application of boundary conditions is necessary for CFD solution accuracy and the problem to be modeled more realistically. The following boundary conditions were applied to the mesh.

• **Velocity inlet**:

The velocity was calculated from the Reynolds number based on the Hydraulic diameter of the channel. The calculated velocity from the Reynolds number was applied to the inlet of the channel. The applied velocity was used to calculate mass flow. The temperature at the inlet, was set at 303 K.

• **Pressure outlet:**

The outlet of the channel was assigned the zero gauge pressure outlet condition which is the default in Fluent. All other values are extrapolated from the interior of the domain.

• **Wall and thermal boundary conditions:**

The wall of the tube was assigned constant temperature boundary condition. A temperature, of 353 K was assigned to this wall to indicate heating at the wall of the test surface. A no slip boundary condition was assigned to all walls that is the velocity of the flow at the wall is zero.

3.7 Solution Methods and Controls:

In this step of Fluent, different solution discretization methods and controls for residual monitors and under relaxation factors can be set.

• **Pressure velocity coupling and discretization scheme:**

The SIMPLE method was chosen for the pressure velocity coupling. The second order upwind spatial discretization scheme was chosen to solve the momentum and energy equations. The second order discretizations were chosen as they give higher order accuracy.

• **Under relaxation factors:**

The default under relaxation factors of 0.3 for pressure, 1 for density 0.7 for momentum and 1 for energy were used. Selections of these under relaxation factors helped in reducing the numerical dissipation errors and achieve faster convergence.

IJERT

(This work is licensed under a Creative Commons Attribution 4.0 International License.)

• **Residuals and surface integrals monitor**:
All residuals were set to 1×10-3 with the exception of residuals for energy equation which were set to 1×10-6 for convergence. The heated surface average Nusselt number and heat transfer coefficients monitors were also created. The surface averaged Nusselt number and surface averaged heat transfer coefficient plots flattened out before convergence was reached.

• **Solution Initialization and calculation:**
The solution was then initialized with all values computed from the inlet face. The solution was then calculated until the surface monitors and the residuals flattened out to the set level of accuracy.

4. NUMERICAL RESULTS AND DISCUSSION

Table 4: Numerical Results for Plain Tube

Re No.	*T_0*	*Nu No.*	*h*	*f*
25799.85	56.2	70.09088	83.2017	0.93185
42998.44	54.4475	105.4702	123.2886	0.91775
60197.03	53.14304	138.0473	159.7974	0.908825
94594.21	51.66001	198.17898	229.3921	0.90877

Table 5: Numerical Results for almond dimple tube

Re No.	*Array of dimple*	*T_0*	*Nu No.*	*h*	*f*
25799.85	**Align**	**64.171**	**83.515**	**126.747**	**1.191536**
	Staggered	**69.958**	**98.663 5**	**176.894**	**1.407652**
42998.25	**Align**	**60.277**	**118.942**	**170.845**	**1.12773**
	Staggered	**65.602**	**137.597**	**228.641**	**1.30461**
60195.30	**Align**	**58.249**	**152.301**	**214.014**	**1.10325**
	Staggered	**63**	**173.389**	**277.38**	**1.25601**
94594.21	**Align**	**52.864**	**196.014**	**246.933**	**0.989075**
	Staggered	**60.54**	**243.366**	**381.273**	**1.229016**

Re No.	*array of dimple*	*h/h_0*	*f/f_0*	*TPF*
25799.85	**Align**	**0.7165**	**0.8465**	**0.8948**
	Staggered	**2.1261**	**1.5103**	**1.2268**
42998.25	**Align**	**0.7472**	**0.8644**	**0.907437**
	Staggered	**1.8545**	**1.4215**	**1.16027**
60195.30	**Align**	**0.7715**	**0.8783**	**0.917183**
	Staggered	**1.7358**	**1.3820**	**1.1276**
94594.21	**Align**	**0.6476**	**0.80477**	**0.865196**
	Staggered	**1.6621**	**1.35238**	**1.11367**

4.1 Heat Transfer:

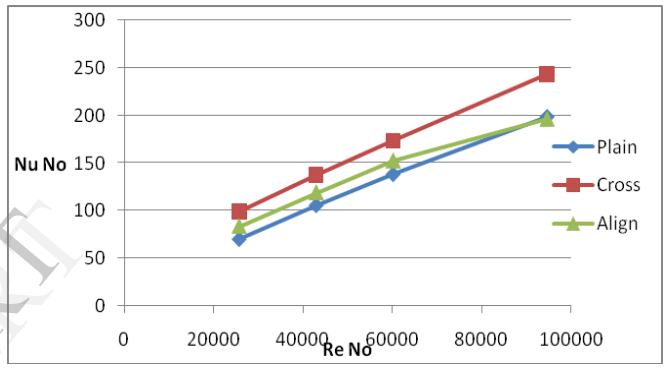

Graph 1: Comparison of Nusselt number staggered and align array geometries Vs Reynolds number

Over the studied Reynolds number range, align almond tube numerically shows slightly higher Nu values than the plain tube; whereas the cross array show distinctively higher Nu values than the plain tubes numerically as well experimentally. For the cross array almond dimple Nusselt number is about 30 to 40 % higher than the plain tube within the Reynolds number range of 25,000 to 95,000. Enhancement efficiency $\eta=h/h_0$ is almost 45 to 50% increases in staggered array dimple tube as compare with align array dimple.

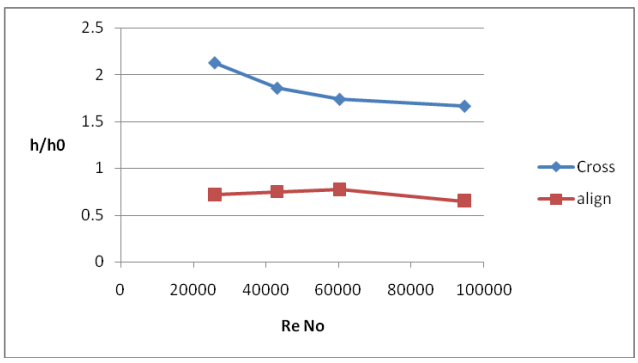

Graph 2: Avg. heat transfer coefficient for align, staggered dimpled array geometry Vs Reynolds number

IJERT

(This work is licensed under a Creative Commons Attribution 4.0 International License.)

4.2 Friction Factors:

The values ΔP are calculated directly from Fluent as the difference between the inlet and outlet pressures of the tube whereas the diameter of the pipe is replaced by the hydraulic diameter of the channel. The friction factor values are calculated and the friction factor ratios with respect to the baseline data for staggered dimpled array geometry and the inline dimpled array geometry are plotted. The values for the two geometries at the Reynolds numbers studied are plotted in figure.

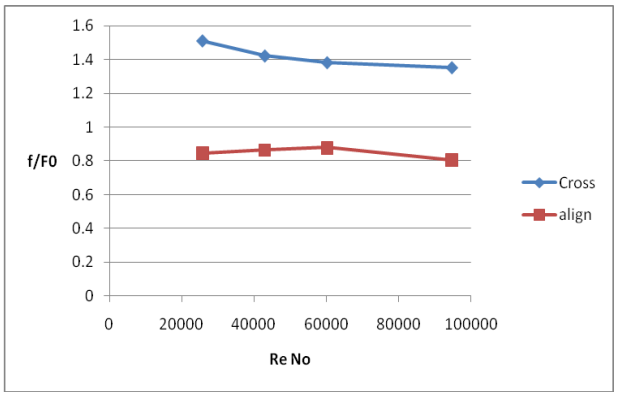

Graph 3: Friction factor ratios for staggered and align dimpled array geometries vs Reynolds number

It can be seen from the plot that dimples do increase friction factors over smooth channels. The friction factor ratios for the staggered dimpled array geometry are more than the inline dimpled array geometry. The friction factors and the pressure drop have a major impact on the thermal performance of the channel. The pressure loss also has to be accounted along with the convective heat transfer coefficient augmentation. The performance of a heat sink can be judged only by taking into account the hydraulic losses and whether the heat transfer coefficient augmentations are worth the hydraulic loss incurred. This can be evaluated by calculating the thermal performance factor which is discussed in the next section.

4.3 Thermal Performance Factor:

For an efficient heat sink, the thermal performance factor has to be greater than 1

The thermal performance factor for the staggered dimpled array and inline dimpled array geometry for the Reynolds number range studied are plotted bellow.

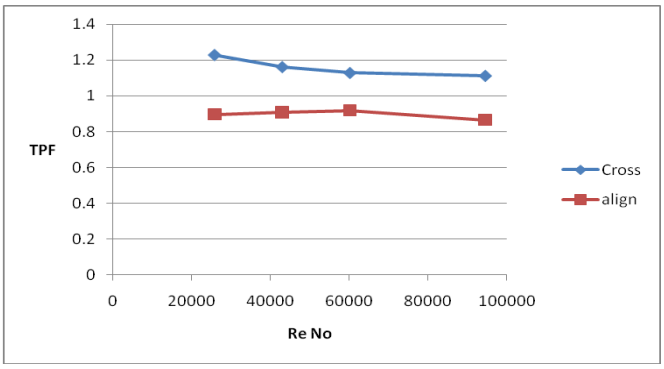

Graph 4: Thermal performance factors for the staggered and align dimpled array Vs Reynolds number

In the Reynolds number range from 25000 to 95000, the thermal performance factor for the inline dimpled array geometry did not rise as much as the one for the staggered dimpled array geometry did.TPF is about 67% higher than align array geometry. In general thermal performance factor follow the same trend of decreasing with increasing Re no as other parameters compare before.

4.4 Flow Structure and Velocity Vectors

The flow structure of the airflow over the dimpled surface was studied by observing the velocity vectors. The post processing capability of Fluent was used to view the velocity vectors. To analyze the flow, the vectors were observed from the span wise and stream wise direction of the channel. This was done to investigate the presence of any secondary flows. From elementary fluid mechanics, a secondary flow is a minor flow superimposed on the primary flow and which is not predicted by simple analytical techniques. The velocity vectors showing the primary flow following the contour of the dimple for both the staggered dimpled array geometry and inline dimpled array geometry for Reynolds numbers 25795 and 94595 are shown in Figure. The velocity contour and static temperature contours, for the staggered and inline array geometries for Reynolds number 25795 and 94594 are shown in Figure.

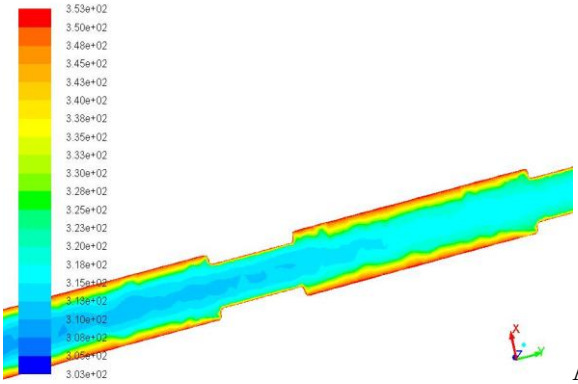

Align

IJERT

(This work is licensed under a Creative Commons Attribution 4.0 International License.)

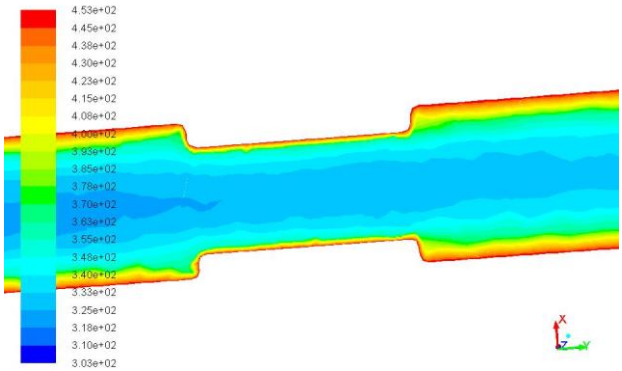

Staggered

Fig.4:Static Temperature Contour Plots for 0.0065kg/sec,Re no=25,795

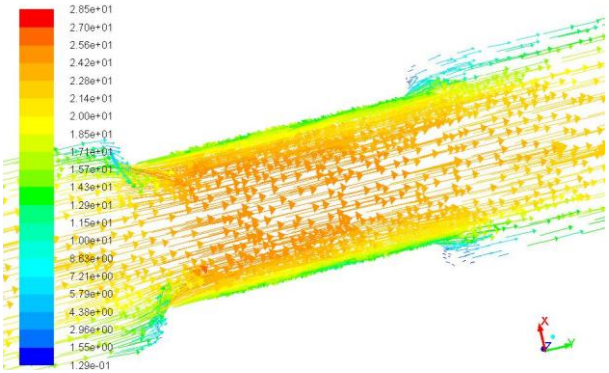

Align

Fig.5:The Velocity Vector Plot for 0.0065 kg/sec, Re no=25,795

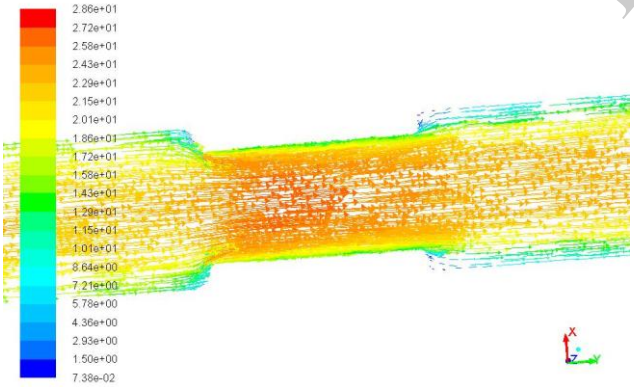

Staggered

Fig.6:The Velocity Vector Plot for 0.0065 kg/sec, Re no=25,795

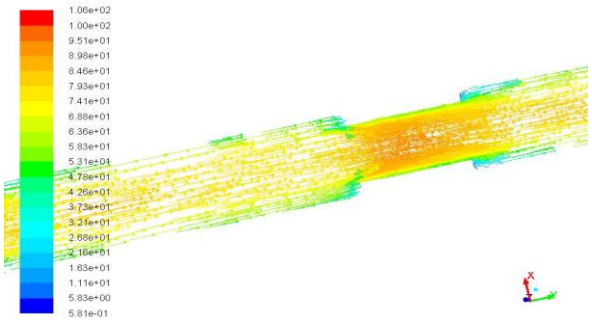

Align

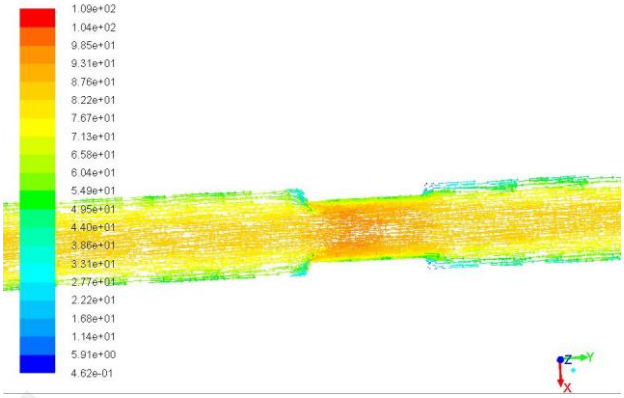

Staggered

Fig.7:The Velocity contour for 0.023997 kg/sec,Re no=94,595

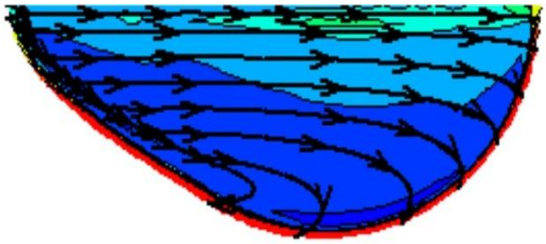

Fig.8: Stream lines on the almond dimple [12]

The majority of the flow inside the almond shape dimple is not reversed. Only small regions of flow reversal are observed in the area adjacent to the upstream portion of the dimple surface. The incoming flow inside the almond dimple directly impinges on a large part of the dimple surface, as shown in Figs.(5,6) The gentle slope of the teardrop dimple's upstream surface is the key behind the flow not experiencing a large separation. The lack of a large flow reversal and the flow impingement along the downstream edge of the dimple contribute to the greater enhancement in the heat transfer on the dimple surface. This observation indicates the most significant difference between the teardrop dimple and the other geometrical shapes of dimples. As the flow travels downstream and leaves the dimple, a full vortex clearly appears above the tube surface in the wake of the dimple, as

IJERT

(This work is licensed under a Creative Commons Attribution 4.0 International License.)

shown in Fig.9 Again, there are two vortices induced by the almond dimple due to the symmetry of the dimple. The vortex pair found in the almond dimple is similar to and slightly stronger than that in the circular dimple. The secondary circulations both at the upstream and downstream end of the dimple are evident from the velocity vectors seen in the span wise direction of the channel. The secondary circulations also increase in strength with increase in Reynolds number. The secondary circulations both at the upstream and downstream end of the dimple are evident from the velocity vectors seen in the span wise direction of the channel. The secondary circulations also increase in strength with increase in Reynolds number. The reattachment in case of these secondary vortexes is also evident. These secondary vortexes therefore contribute in convective heat transfer enhancement [13][21].

5. CONCLUSIONS AND SUMMARY

1. This study focused on investigating whether the use of almond dimples can enhance heat transfer characteristics for a circular tube. Two types of dimpled array geometries on the wall of a tube were tested for four different Reynolds numbers ranging from 25795 to 94594. The dimple geometry were kept constant.

2. Nu no increases about 47 to 60 % in staggered array and 25 to 30% about align array. . Enhancement efficiency obtains by almond shape numerically predicted value about 1 to 2 % and 0.7 to 1 % for staggered and align array respectively.

3. The thermal performance factors were plotted for both the dimpled array geometries. The thermal performance values decreased with increasing Reynolds number values. Again the thermal performance factor values for the staggered dimpled array geometry were more than corresponding inline dimpled array geometry in the Reynolds number range studied.

4. The secondary vortices generated because of the dimple also help in enhancing convective heat transfer coefficient as the vortices help in mixing the hot and cold fluids. Thus, the dimple on the tube found to enhance heat transfer over a plane tube for turbulent airflows. The staggered dimpled array geometry proved to give a better thermal performance than the inline dimpled array.

5. The numerical computation provides reasonably good accuracy in predicting the heat transfer enhancement capability of the cross and align array compared to the plain tube, which is essential to the validation of the computation model since heat transfer prediction is the most important consideration in the heat exchanger device. The gentle slope of the almond dimple's upstream surface is the key behind the flow not experiencing a large separation. The lack of a large flow reversal and the flow impingement along the downstream edge of the dimple contribute to the greater enhancement in the heat transfer on the dimple surface.

6. FUTURE WORK

Every research work always has a definite scope of further activity or extension of previous research work. It is ongoing process of research that the present status of the system can be changed by having certain modification, improvement, innovation, etc

In the present work the geometrical changes are made configuration of dimple arrangement. Whereas the dimples present on the tube are of uniform pitch and dimple print diameter to depth ratio. One can change the depth to dimple print diameter ratio and elongated length of dimple to understand the behavior and influence of variations of dimple geometries present on the circular tube.

The test tube material can be change such as copper, which gives better performance is compared with Dimples shapes variation can be done in such a way which gives maximum heat transfer enhancement with minimum pressure drop penalty.

Further work part of this work will be by making efficient analysis of heat performance parameters, one can develop a correlation for the critical Reynolds number will derive for the circular tube with align and staggered almond shape dimples. Also, friction factor f and Nusselt number correlations will be derive with respect to the Reynolds number and geometric parameters.

IJERT

NOMENCLATURE

D dimple diameter (m)
D_i inner diameter of the tube(m)
f friction factor
h heat transfer coefficient (W/m^2 K)
L length of circular channel (m)
m mass flow rate of the air flow in the channel (kg/m^2)
Nu area averaged Nusselt number of dimple tube
Nu_0 area averaged Nusselt number of tube without dimple
Pr Prandtal number
ΔP pressure drop (Pa)
k fluid thermal conductivity. (W/mK)
Q net heating power (W)
Re Reynolds number
T_{in} inlet fluid temperature (K)
T_{out} outlet fluid temperature (K)
T_w mean wall temperature (K)
ΔT_{lm} log mean temperature difference (K)
q_m mass flow rate (kg/sec)

Greek symbols

ρ density,(kg/m3)
μ dynamic viscosity (Pa.s)

Subscript
in inlet
m mean
out outlet
w Wall

REFERENCES

(This work is licensed under a Creative Commons Attribution 4.0 International License.)

[1] Johann Turnow, Nikolai Kornev,Valery Zhdanov, Egon Hassel, "Flow structures and heat transfer on dimples in a staggered arrangement", *International Journal of Heat and Fluid Flow*, 2012, 35, pp. 168–175.

[2] Yu Rao,Chaoyi Wana, Yamin Xu, "An experimental study of pressure loss and heat transfer in the pinfin-dimple channels with various dimple depths", *International Journal of Heat and Mass Transfer*, 2012, 55, pp. 6723–6733.

[3] C. Bi, G.H. Tang, W.Q. Tao, "Heat transfer enhancement in mini-channel heat sinks with dimples and cylindrical grooves", *Applied Thermal Engineering*, 2013, 55, pp. 121 132.

[4] S.A. Isaev, N.V. Kornev, A.I. Leontiev, E. Hassel,"Influence of the Reynolds number and the spherical dimple depth on turbulent heat transfer and hydraulic loss in a narrow channel", *International Journal of Heat and Mass Transfer* 2010, 53, pp.178-197.

[5] Jonghyeok Lee, Kwan-Soo Lee, "Correlations and shape optimization in a channel with aligned dimples and protrusions", *International Journal of Heat and Mass Transfer*, 2103, 64, pp.444-451. "

[6] Somin Shin, Ki Seon Lee, Seoung Duck Park, Jae Su Kwak, Measurement of the heat transfer coefficient in the dimpled channel:effects of dimple arrangement and channel height", *Journal of Mechanical Science and Technology*, 2009, 23, pp.624-630.

[7] Yu Rao a,Yamin Xu, Chaoyi Wana, "An experimental and numerical study of flow and heat transfer in channels with pin fin-dimple and pin fin arrays", *Experimental Thermal and Fluid Science*, 2012, 38, pp.237-247. "

[8] YuChen, Yong Tian Chew, Boo Cheong Khoo, Enhancement of heat transfer in turbulent channel flow over dimpled surface", *International Journal of Heat and Mass Transfer*, 2012, 55, pp.8100-8121.

[9] Nopparat Katkhaw, NatVorayos, Tanongkiat Kiatsiriroat, Yottana Khunatorn, Damorn Bunturat, AtipoangNuntaphan,"Heat transfer behavior of flat plate having 45^0 ellipsoidal dimpled surfaces", *Thermal engineering*, 2013.

[10] M. Siddique, A. A. Khaled, N. I. Abdulhafiz, and A. Y. Boukhary, "Recent Advances in Heat Transfer Enhancements : A Review Report", *International Journal of Chemical Engineering*, 2010, id.106461.

[11] J.E. Kim, J.H. Doo, M.Y. Ha , H.S. Yoon, C. Son,"Numerical study on characteristics of flow and heat transfer in a cooling passage with protrusion-in-dimple surface", *International Journal of Heat and Mass Transfer*, 2012, 55, pp.7257-7267.

[12] Sumantha Acharya," Experimental and computational study of heat/mass transfer and flow structure of four dimple array in square channel" ,Journal of Turbomachinery, 2012

[13] M.K. Chyu, Y. Yu, H. Ding, J.P. Downs and F.O. Soechting," Concavity enhanced heat transfer in an internal cooling passage*"e, International Gas Turbine & Aeroengine Congress & Exhibition ASME paper 97-GT-437.*

[13] Mohammad A. Elyyan," Heat Transfer Augmentation Surfaces Using Modified Dimples/ Protrusions", Ph.D, Virginia, Blacksburg, 2008.

[14] Cengel, Y. A., Heat and Mass Transfer: A Practical Approch, 3rd ed., Tata McGraw Hill, New York, 2010.

[15] Versteeg, H. K. and Malalasekera, W.,An Introduction to Computational Fluid Ddynamics Finite Volume Method, England, 1995.

IJERT

(This work is licensed under a Creative Commons Attribution 4.0 International License.)